Correction of the distortion in frequency-modulation spectroscopy

Frédéric Du Burck, Olivier Lopez

Correction of the distortion in frequency modulation spectroscopy

F. du Burck, O. Lopez
Laboratoire de Physique des Lasers – Université Paris 13
Avenue Jean-Baptiste Clément, 93430, Villetaneuse, France.

Abstract

A theoretical expression of the detected signal in frequency modulation spectroscopy with a residual amplitude modulation (RAM) is computed. The line shape distortion induced by the RAM is shown to be essentially suppressed for a proper choice of the modulation and detection parameters. The experimental tests are carried out in saturation spectroscopy of I_2 at 514.5 nm. Experimental limitations are analysed.

Key words

Frequency modulation (FM) spectroscopy, residual amplitude modulation (RAM), line shape, laser spectroscopy, ultra-high resolution spectroscopy

I. Introduction

The technique of frequency modulation (FM) spectroscopy was proposed by Bjorklund for the study of weak absorptions and dispersions with a dye laser [1,2] and independently by Drever and Hall for sub-Doppler spectroscopy and for the detection of the reflected field by a Fabry-Perot resonator for laser stabilization [3,4,5]. In FM spectroscopy, a frequency or phase modulation is applied to the probe beam at a frequency large compared to the width of the spectral feature of interest. The Fourier components of the modulated beam, incident on a photodetector, give rise to beat notes at the modulation frequency and its harmonics. In the case of a pure frequency or phase modulation, there is an exact cancellation of the corresponding photocurrents and no signal is detected. If the modulated beam is passed through the sample, the Fourier components experience various attenuations and phase shifts and the cancellation of the photocurrents is destroyed. As a result, a signal may be detected at the modulation frequency or its harmonics.
The FM spectroscopy is of particular interest for high-sensitivity spectroscopy because the modulation frequency may be chosen high enough to operate the detection at a frequency for which the technical noise of the laser is negligible. Moreover, only one frequency component of the modulated beam probes the sample at a time and there is no modulation broadening, which is favourable for the study of narrow lines.
A persistent problem of FM spectroscopy is the sensitivity of the detected signal to the residual amplitude modulation (RAM) generated by the frequency or phase modulator: acousto-optic modulator (AOM), electro-optic modulator (EOM) [6] or current-modulated diode laser [7]. The detection of this amplitude modulation gives a non-zero baseline which may fluctuate in time. Moreover, the technical noise of the laser is transferred at the detection frequency. This noisy background limits the high-sensitive absorption measurements in FM spectroscopy. The RAM also generates a distortion of the detected signal.

Several techniques were proposed in various fields to limit these effects. One can distinguish two approaches according to the RAM of the probe beam is rejected before the interaction with the sample or not.

In the first approach, the beam intensity is monitored by a photodiode at the output of the modulator and an active servo is used to suppress the RAM. The controller may drive a dc voltage applied to the EOM used as modulator located between two polarizers [8]. We have proposed a narrow-band controller which drives the rf input of an AOM [9]. In the field of diode lasers, the RAM rejection may be achieved by an injection technique: the injection-locked slave laser reproduces the frequency spectrum of the current modulated master laser but the RAM is widely decreased [10,11].

In the second approach, no rejection of the RAM before the sample is operated. A first possibility is to choose a proper adjustment of the detection phase to suppress the background contributions due to the RAM [12]. One can also use a spectroscopic scheme less sensitive to the RAM. This is the case of the two-tone FM spectroscopy [13,14] developed in the field of diode laser based gas monitoring [15]. In this technique, the beam is modulated at two distinct frequencies, the difference between them being much smaller than the width of the studied line. The signal is detected at the difference frequency. The suppression of the non-zero baseline and the reduction of the transferred noise may also be achieved by using a reference beam that does not interact with the sample. For instance, we use in the following a balanced detection at the detection frequency (double-beam, double-detector technique). A double-beam, single-detector scheme was described in [16]. Another possibility is to apply an additional modulation to the sample at a frequency smaller than the studied line width. This method is widely used in saturation spectroscopy in which the saturating beam can be amplitude modulated [4,17,18]. In this case, the residual Doppler background is also removed which is an interesting feature for the high precision measurement of position of a Doppler free resonance line. However, in this second approach, it is important to note that the distortion of the line shape still exists since the probe beam is amplitude modulated.

We are interesting in the realisation of optical frequency references based on molecular iodine absorption lines. In particular, narrow lines obtained in the spectral range 500-520 nm, near the dissociation limit of the molecule are promising. The natural width of the hyperfine components of transitions (43-0)P(13) and (43-0)R(15) at 514.5 nm is about 100 kHz [19] and the transitions lying around 500 nm leads to resonances of a few tens of kilohertz wide only [20,21]. The FM spectroscopy is of particular interest for the detection of such narrow lines. Even though it is not the main one, the line shape distortion due to the RAM may be a tedious limitation for the accuracy and reproducibility of frequency references based onto these transitions because it leads to spurious frequency offsets.

In this paper, we show that the distortion of the detected signal due to the RAM may be suppressed by a proper choice of the detected harmonic, the modulation index and the detection phase. In Sect. II, we compute the general expression of the detected signal in FM spectroscopy with a RAM and we show how to choose the modulation and detection parameters to reject the distortion of the line shape. In Sect. III, we describe our experimental set-up for the saturation spectroscopy of I_2 at 514.5 nm. The probe beam is simultaneously frequency modulated and amplitude modulated at 2.1 MHz with controlled characteristics by an AOM. The reductions of the background signal and of the transferred noise are achieved either with a simple balanced detection at the detection frequency or with the technique of the additional modulation of the sample. In Sect. IV, we show experimentally that the distortion of the line shapes detected in saturation spectroscopy can be essentially cancelled and that symmetrical line shapes are recovered even with a large amplitude modulation of the probe beam. We have also studied the sensitivity of the pseudo-centre of the line to the adjustment of the modulation index and of the detection phase. Finally, we conclude in Sect. V.

II. Theoretical analysis

II.1 General expression of the detected signal

One considers the propagation of a laser beam through a cell of length L which contains the molecular vapour under study (the sample). The beam is frequency modulated at the angular frequency ω_m and amplitude modulated at the same fundamental frequency. The field is of the form

$$e(t) = \sum_k M_k e^{ik\omega_m t} \times e^{i[\omega_c t + \beta \sin(\omega_m t)]} \quad (1)$$

where ω_c is the angular frequency of the optical carrier, β is the modulation index and $M_k = m_k e^{i\psi_k}$ is the k-th coefficient of the Fourier spectral series of the amplitude modulation (AM) signal. It is assumed that $M_0 = 1$ (the amplitude of the optical carrier is taken as unity) and one notes that $M_{-k} = M_k^*$ because the AM signal is real. Using the Fourier expansion of the FM signal

$$e^{i[\omega_c t + \beta \sin(\omega_m t)]} = \sum_p J_p(\beta) e^{i(\omega_c + p\omega_m)t} \quad (2)$$

in which $J_n(.)$ is the n-th order Bessel function, the field simultaneously amplitude and frequency modulated in (1) may be written

$$e(t) = \sum_p h_p e^{i(\omega_c + p\omega_m)t} \quad (3)$$

with

$$h_p = \sum_k M_k J_{p-k}(\beta) \ . \quad (4)$$

It can be noted that the cases of a pure frequency modulated field and a pure amplitude modulated field are given by (3), making $h_p = J_p(\beta)$ and $h_p = M_p$ respectively. Through the cell, each spectral component of the field (3) at angular frequency ω experiences an absorption and a phase shift (Fig. 1). The effect of the medium on the beam is thus described by the factor

$$F(\omega) = e^{-T(\omega) - \theta} \quad (5)$$

with

$$T(\omega) = \frac{\alpha(\omega)L}{2} + i\frac{\omega n(\omega)L}{c} \ . \quad (6)$$

$\alpha(\omega)$ is the absorption coefficient of the medium and $n(\omega)$ is the index of refraction. $T(\omega)$ shows resonances for each molecular transition frequency. The complex number θ is introduced to take possible constant attenuation and phase shift into account. For instance, θ may represent the linear absorption in saturation spectroscopy if this one can be considered as a constant on the scale of the FM spectrum. The emerging field is then

$$s(t) = \sum_p h_p F_p e^{i(\omega_c + p\omega_m)t} \quad (7)$$

with $F_p = F(\omega_c + p\omega_m)$. Finally, the n-th harmonic detection with the phase φ operated on the beam intensity is proportional to the dc component of $s(t)s^*(t) \times \cos(n\omega_m t + \varphi)$. This leads to a detected signal proportional to

$$S_{det} = \frac{1}{2}\sum_p h_p F_p \left(h^*_{p+n} F^*_{p+n} e^{i\varphi} + h^*_{p-n} F^*_{p-n} e^{-i\varphi} \right). \quad (8)$$

The line shape is obtained by scanning the frequency of the optical carrier ω_c around the frequency of the molecular transition of interest ω_0. In the following, this frequency shift is noted Δ:

$$\Delta = \omega_c - \omega_0. \quad (9)$$

We are interesting here in the detection of a weak resonance ($|T(\omega)| << 1$). Expression (5) is thus approximated by

$$F(\omega) \approx (1 - T(\omega)) \times e^{-\theta} \quad (10)$$

and the detected signal (8) becomes to first order

$$S_{det} = \frac{\Theta}{2}\sum_p h_p \left(h^*_{p+n} e^{i\varphi} + h^*_{p-n} e^{-i\varphi} \right) - \Theta \sum_p Re\left\{ T_p h_p \left(h^*_{p+n} e^{i\varphi} + h^*_{p-n} e^{-i\varphi} \right) \right\} \quad (11)$$

with $T_p = T(\omega_c + p\omega_m)$ and $\Theta = \left| e^{-\theta} \right|^2$. We will see in Sect. II.2 that the first term in (11) corresponds to the dc background. The second term is the sum of components centred at $\Delta = \pm p\omega_m$. For a modulation frequency ω_m much higher than the line width, these components are well separated from each other and the expression of the detected signal around $\Delta = 0$ may be simplified as

$$S_{\text{det}} = \frac{\Theta}{2}\sum_p h_p \left(h^*_{p+n} e^{i\varphi} + h^*_{p-n} e^{-i\varphi} \right) - \Theta \,\text{Re}\left\{ T_0 h_0 \left(h^*_n e^{i\varphi} + h^*_{-n} e^{-i\varphi} \right) \right\}. \quad (12)$$

Equations (11) and (12) are the basic expressions used to analyse the effect of the RAM in FM spectroscopy.

II.2 The dc background

The detection of a spurious amplitude modulation leads to a dc background. This background, corresponding to the signal detected with no gas in the cell, is computed by making $F(\omega) = 1$ in (8). When the sample is present, the background has to be multiplied by Θ as it is seen in (11) or (12). Using (4) and the following summation property of Bessel functions

$$\sum_p J_p(\beta) J_{p+q}(\beta) = \delta_{0q} \quad (13)$$

where δ_{ab} is the Kronecker's symbol, the background detected with a phase φ may be written

$$S_{bg}(\varphi) = \frac{1}{2}\sum_k M_k \left(M^*_{k+n} e^{i\varphi} + M^*_{k-n} e^{-i\varphi} \right). \quad (14)$$

Let us note that in the case of a pure frequency modulated field ($M_0 = 1$ and $M_k = 0$, $|k| > 0$), the non-zero background vanishes.

Generally, the amplitude m_k of the Fourier components of the AM signal rapidly decreases with *k*. It is seen in (14) that in this case, the detection of a higher harmonic *n* leads to a lower background. For instance, in our experimental set-up, a 30 % amplitude modulation of the field at $\omega_m / 2\pi = 2.1\,\text{MHz}$ is achieved by a sinusoidal modulation of the beam intensity at ω_m. Because of the quadratic relation between field and intensity, components at $2\omega_m$, $3\omega_m$, … also appear. One can compute the coefficients of the Fourier series of the AM signal : $M_0 = 1$, $M_1 = 0.15\, e^{i\psi}$, $M_2 = 0.01\, e^{i(2\psi+\pi)}$, $M_3 = 0.0014\, e^{i3\psi}$, … The maximum background

detected with $n = 2$, 3, 4, 5 represents respectively 10.1 %, 1.4 %, 0.12 % and 0.01 % of the maximum background detected with $n = 1$.

II.3 Detection of the signal without RAM

In the case of a pure frequency modulation, the expressions of the detected signal (11) and (12) become

$$S_{det} = -\Theta \sum_p Re\left\{T_p J_p(\beta)\left(J_{p+n}(\beta)e^{i\varphi} + J_{p-n}(\beta)e^{-i\varphi}\right)\right\} \quad (15)$$

and

$$S_{det} = -\Theta\, Re\left\{T_0 J_0(\beta)\left(J_n(\beta)e^{i\varphi} + J_{-n}(\beta)e^{-i\varphi}\right)\right\} . \quad (16)$$

When *n* is even, $J_{-n}(\beta) = J_n(\beta)$ and (16) may be rewritten as

$$S_{det} = -2\Theta J_0(\beta) J_n(\beta)\, Re\{T_0\} cos(\varphi) \quad (17)$$

which corresponds to an absorption-like line shape centred at $\Delta = 0$. The in-phase detection gives the maximum signal. When *n* is odd, $J_{-n}(\beta) = -J_n(\beta)$ and the detected signal becomes

$$S_{det} = 2\Theta J_0(\beta) J_n(\beta)\, Im\{T_0\} sin(\varphi) \quad (18)$$

which is a dispersion-like line shape centred at $\Delta = 0$. The maximum signal is obtained with a quadrature detection.

Let us note at last that when the sum in (15) is limited to components $J_0(\beta)$, $J_{\pm 1}(\beta)$, $J_{\pm 2}(\beta)$, this expression corresponds to the detection of the photocurrent components at ω_m ($n = 1$) and $2\omega_m$ ($n = 2$) computed in [22] (expressions (6) and (8)). Expression (16) corresponds to the detection of the component at ω_m derived in [2].

II.4 Distortion due to the RAM

From expressions (12) and (14), the detected signal is

$$S_{\det} = \Theta S_{bg}(\varphi) - \Theta\, \mathrm{Re}\left\{T_0 h_0\left(h_n^* e^{i\varphi} + h_{-n}^* e^{-i\varphi}\right)\right\} . \quad (19)$$

Considering the in-phase detection with *n* even, the detected signal (19) takes the form

$$S_{det} = \Theta S_{bg}(0) - 2\Theta J_0(\beta) J_n(\beta)\, Re\{T_0 \kappa\} \quad (20)$$

and for the quadrature detection with *n* odd

$$S_{det} = \Theta S_{bg}(\pi/2) + 2\Theta J_0(\beta) J_n(\beta)\, Im\{T_0 \kappa\} . \quad (21)$$

For $J_0(\beta) J_n(\beta) \neq 0$, the coefficient κ appearing in (20) and (21) is given by

$$\kappa = \frac{1}{2 J_0(\beta) J_n(\beta)} \sum_k M_k J_{-k}(\beta) \sum_l \left(M_l^* + (-1)^l M_l\right) J_{n-l}(\beta) . \quad (22)$$

In the general case, κ is a complex number and the "useful" signal superimposed onto the dc background is the result of a "mixing" of the real and imaginary parts of T_0. As a result, the symmetry of the detected signal vanishes and the line shape is distorted. It is shown in Appendix 1 that the imaginary part of κ may be written as a sum of the odd coefficients of the Fourier series of the AM signal and a double sum of cross terms mixing even and odd coefficients (expression (A3)).

Let us consider now an AM signal with a single component at ω_m. We only retain this term in (1) and we have the field

$$e(t) = \left[1 + \mu\, cos(\omega_m t + \psi)\right] e^{i[\omega_c t + \beta\, sin(\omega_m t)]} \quad (23)$$

with $\mu = 2m_1$ and $\psi = \psi_1$. From expression (A5) of Appendix 1, the coefficient κ is in this case

$$\kappa = 1 + \frac{J_1(\beta)}{J_0(\beta)} \times \frac{J_{n+1}(\beta) - J_{n-1}(\beta)}{2J_n(\beta)} \mu^2 \sin^2(\psi) - i\left(\frac{J_1(\beta)}{J_0(\beta)} - \frac{J_{n+1}(\beta) - J_{n-1}(\beta)}{2J_n(\beta)} \right) \mu \sin(\psi). \quad (24)$$

It is remarkable in (24) that the imaginary part of κ may be equal to 0 independently of the degree of amplitude modulation μ and of the phase difference between the amplitude and the frequency modulation ψ. Consequently, the detected line shape is symmetrical with respect to $\Delta = 0$ for any value of μ or ψ when

$$\frac{J_1(\beta)}{J_0(\beta)} - \frac{J_{n+1}(\beta) - J_{n-1}(\beta)}{2J_n(\beta)} = 0 \ . \quad (25)$$

Our experimental set-up described in Sect. III is designed to detect the third harmonic. From Table 1 of Appendix 1, condition (25) may be achieved for $n = 3$ with $\beta = 3.544$.

Let us note that in practice, the components at $k\omega_m$ with $|k| > 1$ are not exactly equal to zero and one can only say that the term at ω_m of the Fourier series of the AM signal is considerably larger than the other terms ($m_k << m_1$ for $|k| > 1$). For instance, in the case of the sinusoidal modulation of the beam intensity considered in Sect. II.2, m_2 is already 15 times smaller than m_1. For the parameters used in our experiment ($n = 3$, $\varphi = \pi/2$, $\beta = 3.544$), which lead to cancel the term of the imaginary part of κ due to the ω_m component of the AM signal, one can compute from (22) the contributions of other components. It is found that the maximum contribution of the components at $3\omega_m$ to the imaginary part of κ represents 0.46 % of its real part and that of the cross term due to components at ω_m and $2\omega_m$ is 0.25 %. The distortion of the line shape is thus essentially associated to the amplitude modulation at frequency ω_m and the other terms may be neglected.

A condition similar to (25) was found by Bava and Massari [23] in the study of the detection of the light reflected from a Fabry-Perot interferometer. In this case, the cavity reflection coefficient plays the role of *F(ω)* in (5).

This result may also be compared to the case of high-frequency modulation transfer technique in stimulated Raman spectroscopy in which the general expression of the detected signal is derived from a fourth order development of the density matrix equations [24]. It is shown in ref. [25] that condition (25) leads also to cancel the distortion of the line shape due to the RAM.

Let us recall that condition (25) is established in the case of a modulation frequency substantially larger than the line width. As a matter of fact, it is derived from expression (12) in which the component of the detected signal centred at $\Delta = 0$ is considered. Consequently, condition (25) leads to suppress the distortion of this signal only. If the modulation frequency is not very high compared to the line width, a weak distortion of the detected line shape may persist due to the components centred at $\Delta = \pm\omega_m, \pm 2\omega_m, \ldots$ This is illustrated by Fig. 2 in which $T(\omega)$ is taken as a complex Lorentzian with a half width at half maximum $HWHM = g$. The modulation and detection parameters are $n = 3$, $\beta = 3.544$, $\varphi = \pi/2$. A 30 % amplitude modulation is applied in phase with the FM signal ($\mu = 0.3$, $\psi = 0$). In Fig. 2(a), the components centred at $\Delta = -\omega_m$, 0 and $+\omega_m$ are plotted in solid lines for a

modulation frequency $\omega_m = 10g$. The broken line is the sum of the three previous curves. One can see that the distortion of components centred at $\Delta = \pm\omega_m$ leads to a shift of the line centred at $\Delta = 0$. Fig 2(b) shows the line shapes near $\Delta = 0$ for various modulation frequencies computed from the "complete" expression (11) (without the dc background). Although condition (25) is observed, it is seen that a shift of the line shape appears when the modulation frequency is not sufficient.

III. Experimental set-up

An acousto-optic modulator (AOM) is a convenient device to produce a laser beam simultaneously amplitude and frequency modulated [25]. However, the modulation frequency cannot exceed a few megahertz because of the AOM transmission band. We choose a modulation frequency $\omega_m / 2\pi = 2.1\,\text{MHz}$, the larger possible value for our device, and we detect the strong and narrow resonances obtained in saturation spectroscopy of molecular iodine at 514.5 nm. In particular, the natural width of the hyperfine component a_2 of the transition (43-0)P(13) is about 50 kHz [19]. The technical noise of our set-up extends up to a few megahertz and we found experimentally that the noise at 2.1 MHz is only 10-15 dB above the shot noise limit. On the other hand, this modulation frequency is much smaller than the frequency separation between the main lines of the hyperfine structure (a few tens of megahertz) [26], which avoids interferences between the detected lines.

III.1 The spectrometer

The spectrometer is shown in Fig. 3. A monomode Ar^+ laser is prestabilised on a Fabry-Perot resonator mode and locked to the line a_2 of the transition (43-0)P(13) in iodine, detected with the first harmonic of the saturated absorption signal. The iodine pressure in the 50 cm long sealed cell used for the laser stabilisation (not seen in Fig. 3) is about 3 Pa. The frequency jitter of the laser is estimated at a few tens of kilohertz. The laser beam is split into the probe beam and the saturating beam which are frequency shifted by AOM1 ($\Omega_1 / 2\pi = 250\,\text{MHz}$) and AOM2 ($\Omega_2 / 2\pi = 230\,\text{MHz}$) respectively. A frequency shift is introduced in the stabilisation scheme to balance Ω_1 and Ω_2. The probe beam is modulated at $\omega_m / 2\pi = 2.1\,\text{MHz}$ by AOM1. The frequency scanning is only applied to the saturating beam (AOM2). Consequently, noting Γ the line width of the molecular resonance, the detected signal is composed of 2Γ wide resonances located at $\pm p\omega_m$ with $p = 0,\pm1,\pm2,...$ [27,22]. Modulators AOM1 and AOM2 are located at the focus of lenses L1 and L2 respectively, ($f = 5$ cm) in order to avoid the splitting of the frequency components of the probe beam and the angular deviation of the saturating beam during the frequency scanning. In order to improve the wave fronts quality, the beams with crossed linear polarizations are superimposed before crossing a telescope with a 10 μm diameter pinhole. The diameter of the beams at the output of the telescope is 6 mm. Both polarizations are then split by a polarizing beamsplitter cube (BSC), and the probe and saturating beams are propagating in opposite directions through the cell. The cell is continuously pumped during the measurements, and the iodine pressure is controlled by thermostabilization of a cold finger. The cell is 4 m long and the interaction length between the beams and the iodine vapour is 8 m.

III.2 Modulation and detection

The simultaneous amplitude and frequency modulated signal applied to AOM1 is produced by a home made device. The modulation index β can be adjusted between 0 and 4, observing the spectrum of the FM signal with a spectrum analyser. According to Carson's rule [28], for $\beta = 4$ the spectrum of the FM signal extends on about 20 MHz around 250 MHz. The amplitude modulation is added to the FM signal using a double-balanced mixer. Five values of the phase difference between the amplitude and the frequency modulations ($\psi = 65$, 95, 125, 155, 185 degrees) may be selected by switches.
The modulated signal is applied to AOM1 (AA SHT 250 A&A) with a rf power chosen such as the AOM works in the linear part of its characteristic. The frequency response of AOM1 in a frequency band of 20 MHz centred on 250 MHz shows fluctuations smaller than 2 dB. When a pure FM signal is applied to AOM1 with $\beta \approx 3.5$, the probe beam shows an amplitude modulation of a few % at ω_m. When a 30 % amplitude modulation is added ($\mu = 2m_1 = 0.3$), besides the component at ω_m, the beam intensity shows spectral components at $2\omega_m$ and $3\omega_m$ with a size equal respectively to 20 % and 4 % of the size of the ω_m component. A third-harmonic detection is operated on the probe beam with a rf lock-in amplifier (SR844 Stanford Research System).
We use two techniques for the suppression of the non-zero background due to the amplitude modulation of the probe beam and to the linear absorption in iodine. Firstly, we use a balanced detection at the detection frequency. The probe beam is split into two beams with roughly the same power. Both beams propagate through the cell, but only one of them interacts with the saturating beam. The other one is a reference beam which only probes the linear absorption. The probe beam, after suppression of the saturating beam, and the reference beam are measured by two photodetectors with equivalent characteristics (PD1 and PD2). The difference between both signals is obtained at the output of a rf power splitter (PS). The difference between optical paths are balanced by an accurate adjustment of the coaxial length at the output of the photodetectors. An optical attenuator (Opt. att.) is located on the probe beam and an electrical attenuator (RF att.) is at the output of the reference photodetector PD2. Before the experiment, an amplitude modulation is applied to the probe beam at the detection frequency ($3\omega_m / 2\pi = 6.3$ MHz) and the corresponding components observed at the output of PS on a spectrum analyser are minimized by adjusting the attenuators. In particular, the component at $3\omega_m$ is rejected by more than 40 dB, which essentially cancels the low frequency noise transferred at the detection frequency. However, we observe a slight dc background with a slow drift superimposed to the detected signal. This offset is compensated without the saturating beam before each acquisition in order to take the linear absorption as a zero.
For the precise determination of the zero crossing (Sect. IV.2), we also use the usual technique of additional modulation of the sample: the saturating beam is amplitude modulated at 5 kHz and the output signal of the rf detection is demodulated by a low-frequency lock-in amplifier.

IV. Experimental results

The third harmonic detection of the hyperfine component a_2 of the P(13) line of iodine at 514.5 nm is operated in FM spectroscopy. The optimum detection phase $\varphi = \varphi_0 = 90°$ is adjusted by cancelling the quadrature signal at $\Delta = 0$ without any added amplitude modulation.

IV.1 Distortion due to the RAM

Fig. 4 shows line shapes recorded with the modulation index $\beta = 2.8$, that is to say, a value rather different from the optimum value $\beta_0 = 3.544$ leading to the correction of the distortion. The background signal is suppressed using a balanced detection at $3\omega_m$ as mentioned earlier. Signal (a) is obtained without any amplitude modulation. It shows an odd symmetry and it is centred at $\Delta = 0$. The broken line represents the fit of experimental data with the imaginary part of a complex Lorentzian (expression (18)). The half width at half maximum is $HWHM = 152\,\text{kHz}$ (that is to say a molecular line width $\Gamma = 76\,\text{kHz}$). The solid line is the theoretical line shape computed with expression (15) which takes into account the components of the detected signal centred at $\pm p\omega_m$. Both curves are identical around $\Delta = 0$ but a slight deviation appears in the wings because of the signals centred at $\Delta = \pm\omega_m$ which are neglected in expression (18).
Signals (b) are recorded with a 30 % amplitude modulation applied nearly opposite in phase ($\psi = 185°$) with the FM signal. As shown in Appendix 1, the signal detected with $\varphi = 90°$ is practically not distorted in this case. This signal shows an offset due to the components centred at $\Delta = \pm\omega_m$ (see Fig. 2 in Sect. II.4). This can be verified by comparing the theoretical line shape computed by expression (11) (solid line), taking into account the contributions of the signals centred at $\Delta = \pm p\omega_m$, and that computed by expression (12) (broken line), in which only the signal centred at $\Delta = 0$ is considered (in both cases, the non zero background is suppressed). The amplitude modulation gives rise here to a strong signal with an even symmetry detected with $\varphi = 180°$, that is to say a detection phase almost in phase with the AM signal.
For signals (c), a 30 % amplitude modulation is applied nearly in quadrature ($\psi = 95°$) with the frequency modulation. The signal detected with $\varphi = 180°$ is much smaller than in the previous case because the detection is operated almost in quadrature with the AM signal. The signal detected with $\varphi = 90°$ is now strongly distorted because of the amplitude modulation. The solid and broken lines are the theoretical line shapes computed by (11) and (12) respectively as in the previous case.
Fig. 5 shows the signals obtained with the detection phase $\varphi = \varphi_0 = 90°$ and the modulation index $\beta = \beta_0 = 3.544$, without any amplitude modulation, or with a 30 % amplitude modulation applied nearly in quadrature ($\psi = 95°$) or nearly opposite in phase ($\psi = 185°$) with the frequency modulation. The line width is $HWHM = 130\,\text{kHz}$ ($\Gamma = 65\,\text{kHz}$). As shown by the theoretical analysis, the distortion due to the amplitude modulation essentially vanishes and the three line shapes are practically centred at $\Delta = 0$.

IV.2 Shift of the pseudo-centre of the line

In practice, the frequency for which the line shape goes through zero often corresponds to the estimate centre of the resonance (pseudo-centre), for instance, when it is used as a frequency reference for the stabilization of a laser source. It is therefore important to study the sensitivity of the pseudo-centre to the adjustment of the modulation index β and the phase detection φ around their ideal values β_0 and φ_0. A theoretical value of the deviation δ of the zero crossing is derived in Appendix 2 (expression (A11)).
For an experimental study, it is of course essential to perfectly cancel the dc background. For this purpose, we use the technique of sample modulation rather than the technique of balanced

detection. As noted above, this latter is not stable enough for these measurements. The deviations δ of the pseudo-centre of the line associated to the deviation $\Delta\beta = \beta - \beta_0$ of the modulation index and $\Delta\varphi = \varphi - \varphi_0$ of the phase detection are measured for a line width $HWHM = 130$ kHz and a 30 % amplitude modulation.

Let us note first that, in our set-up, even for $\Delta\beta = 0$ and $\Delta\varphi = 0$, a slight shift of the pseudo-centre appears when the amplitude modulation is applied. This is due to the proximity of the components of the detected signal centred at $\pm\omega_m$ which are not symmetrical with respect to $\Delta = 0$, as noted above (Sect. II.4). The deviations of the zero crossing measured for various phase shifts ψ between the amplitude and the frequency modulations do not exceed $\delta = \pm 2$ kHz. This value is confirmed by simulations carried out with the theoretical line shape (11).

The deviation δ versus $\Delta\varphi$ with the modulation index fixed to β_0 is plotted in Fig. 6. A quasi-linear dependence is observed with a negative slope (-0.61 kHz/degree) for $\psi = 185°$ and with a slight positive slope (0.04 kHz/degree) for $\psi = 95°$. In each case, the deviation given by expression (A11) is plotted in solid line. For $\psi = 185°$, the slope given by expression (A12) is $(\partial\delta / \partial\varphi)_{\varphi_0,\beta_0} = -0.57$ kHz/degree which is in good agreement with the experiment, but the experimental values are shifted by about 1.5 kHz compared to the theoretical curve. For $\psi = 95°$, expression (A12) gives a negative slope ($(\partial\delta / \partial\varphi)_{\varphi_0,\beta_0} = -0.05$ kHz/degree), contrary to the experimental one. The deviations from experimental data observed in both cases are explained by the proximity of the components near $\Delta = \pm\omega_m$. The broken lines are computed by the theoretical line shape (11), taking into account these components. An excellent agreement with experimental data is obtained.

Fig. 7 shows the deviation δ versus $\Delta\beta$ measured with the ideal phase detection φ_0. As in Fig. 6, the solid lines are the deviations computed by expression (A11) and the broken lines are the deviations derived from the theoretical line shape (11). A good agreement is obtained for $\psi = 185°$, but the experimental deviation is smaller than the theoretical one for $\psi = 95°$. This feature may be attributed to the amplitude modulation at $2\omega_m$ and $3\omega_m$ observed at the output of AOM1. Indeed, these components introduced in the line shape (11) with proper phases leads to a decrease of the deviation δ in the case $\psi = 95°$.

V. Conclusion

We have proposed in this paper a complete analysis of the dc background and the distortion induced in FM spectroscopy by any amplitude modulation. When the size of one of the components of the Fourier series of the AM signal is considerably larger than the others, we have shown how the distortion can be cancelled by a proper choice of the detected harmonic, the modulation index and the detection phase. Even with a strong amplitude modulation, we have confirmed experimentally that line shapes essentially not distorted may be obtained in saturation spectroscopy. We have also studied the sensitivity of the correction to the adjustment of the modulation index and to the detection phase around their optimum values. This technique may be associated with a method of background suppression like the saturating beam modulation for ultra-high resolution spectroscopy or for precision servo locking of the source onto a sharp reference line.

In our experiment, the probe beam is frequency modulated at 2.1 MHz by an AOM. As noted above, although this frequency is sufficient for the technical noise spectrum, the correction of the distortion is limited due to the proximity of the components of the detected signal centred

at $\pm\omega_m$. It would be better to use a higher modulation frequency (from Fig. 2, a modulation frequency 20-30 times higher than the line width seems to be a good choice). This would be possible with our AOM, using a double pass scheme. An EOM which can reach higher modulation frequencies could also be used, but it must be noted that a modulation index such as $\beta_0 = 3.544$ required for the correction of the distortion is more difficult to achieve with this device.

VI. Appendix 1: Computation of κ

Putting together the coefficients of the Fourier spectral series of the AM signal with opposite indexes in (22), κ may be rewritten under the form

$$\kappa = 1 + \sum_{k=1}^{\infty}\left(\varepsilon_k \frac{J_k(\beta)}{J_0(\beta)}) + \frac{\varepsilon_k^* J_{n+k}(\beta) + \varepsilon_k J_{n-k}(\beta)}{2J_n(\beta)} \right) + \sum_{k=1}^{\infty}\sum_{l=1}^{\infty} \varepsilon_k \frac{J_k(\beta)}{J_0(\beta)}) \times \frac{\varepsilon_l^* J_{n+l}(\beta) + \varepsilon_l J_{n-l}(\beta)}{2J_n(\beta)} \quad \text{(A1)}$$

with

$$\varepsilon_k = M_k^* + (-1)^k M_k \,. \quad \text{(A2)}$$

Noting that $\varepsilon_k = 2m_k\, cos(\psi_k)$ for k even and $\varepsilon_k = -i2m_k \sin(\psi_k)$ for k odd, one can separate the real and imaginary part of κ:

$$\begin{aligned}
\kappa = 1 &+ \sum_{k=1}^{\infty}\left(\frac{J_{2k}(\beta)}{J_0(\beta)} + \frac{J_{n+2k}(\beta) + J_{n-2k}(\beta)}{2J_n(\beta)} \right) 2m_{2k} \cos(\psi_{2k}) \\
&+ \sum_{k=1}^{\infty}\sum_{l=1}^{\infty} \frac{J_{2k}(\beta)}{J_0(\beta)} \times \frac{J_{n+2l}(\beta) + J_{n-2l}(\beta)}{2J_n(\beta)} 4m_{2k} m_{2l} \cos(\psi_{2k}) \cos(\psi_{2l}) \\
&+ \sum_{k=1}^{\infty}\sum_{l=1}^{\infty} \frac{J_{2k-1}(\beta)}{J_0(\beta)} \times \frac{J_{n+2l-1}(\beta) - J_{n-2l+1}(\beta)}{2J_n(\beta)} 4m_{2k-1} m_{2l-1} \sin(\psi_{2k-1}) \sin(\psi_{2l-1}) \\
&- i\sum_{k=1}^{\infty}\left(\frac{J_{2k-1}(\beta)}{J_0(\beta)} - \frac{J_{n+2k-1}(\beta) - J_{n-2k+1}(\beta)}{2J_n(\beta)} \right) 2m_{2k-1} \sin(\psi_{2k-1}) \\
&+ i\sum_{k=1}^{\infty}\sum_{l=1}^{\infty} \frac{J_{2k}(\beta)}{J_0(\beta)} \times \frac{J_{n+2l-1}(\beta) - J_{n-2l+1}(\beta)}{2J_n(\beta)} 4m_{2k} m_{2l-1} \cos(\psi_{2k}) \sin(\psi_{2l-1}) \\
&- i\sum_{k=1}^{\infty}\sum_{l=1}^{\infty} \frac{J_{2k-1}(\beta)}{J_0(\beta)} \times \frac{J_{n+2l}(\beta) + J_{n-2l}(\beta)}{2J_n(\beta)} 4m_{2k-1} m_{2l} \sin(\psi_{2k-1}) \cos(\psi_{2l})
\end{aligned} \quad \text{(A3)}$$

Expression (A3) shows that the imaginary part of κ, which gives rise to the distortion of the line shape, is due to the odd components of the AM signal, either directly (sum of m_{2k-1}) or mixed with the even components (sum of $m_{2k} m_{2l-1}$ and $m_{2k-1} m_{2l}$). Moreover, when the phase ψ_{2k-1} of an odd component is 0 or π, it does not contribute to the distortion.

Let us consider now the case of an amplitude modulation at frequency $K\omega_m$ (K odd integer). For this purpose, one makes $M_k = 0$ for $|k| \neq 0, K$ in the expression of the field (1). The field becomes

$$e(t) = \left(M_K^* e^{-iK\omega_m t} + 1 + M_K e^{iK\omega_m t} \right) \times e^{i[\omega_c t + \beta \sin(\omega_m t)]} \,. \quad \text{(A4)}$$

From (A3), κ is given by

$$\kappa = 1 + \frac{J_K(\beta)}{J_0(\beta)} \times \frac{J_{n+K}(\beta) - J_{n-K}(\beta)}{2J_n(\beta)} 4m_K^2 \sin^2(\psi_K)$$
$$- i\left(\frac{J_K(\beta)}{J_0(\beta)} - \frac{J_{n+K}(\beta) - J_{n-K}(\beta)}{2J_n(\beta)} \right) 2m_K \sin(\psi_K) . \qquad \text{(A5)}$$

Expression (A5) shows that the imaginary part of κ may be equal to 0 independently of $M_K = m_K e^{i\psi_K}$ by choosing β such as

$$\frac{J_K(\beta)}{J_0(\beta)} - \frac{J_{n+K}(\beta) - J_{n-K}(\beta)}{2J_n(\beta)} = 0 . \qquad \text{(A6)}$$

The distortion of the detected line shape then vanishes. Some values of β which are solutions of equation (A6) are given in Table 1 for various *n* and *K*.

V. Appendix 2: Shift of the zero crossing due to $\Delta\beta$ and $\Delta\varphi$

One considers here the detection of the signal with an odd harmonic *n* in the case of a high modulation frequency and a perfect rejection of the dc background. The detected line shape (12) takes the form

$$S_{det} = -\Theta \, Re\left\{ T_0 h_0 \left(h_n^* e^{i\varphi} + h_{-n}^* e^{-i\varphi} \right) \right\} . \qquad \text{(A7)}$$

As was shown in Sect. II, for a detection phase φ and a modulation index β exactly equal to their ideal values $\varphi_0 = 90°$ and β_0 given in Table 1 (for instance $\beta_0 = 3.544$ for $n = 3$), the line shape shows an odd symmetry around $\Delta = 0$ even for a residual amplitude modulation at the modulation frequency $K\omega_m$.

It is assumed now that φ and β deviate from φ_0 and β_0. In (A7), T_0 is multiplied by the complex number $h_0\left(h_n^* e^{i\varphi} + h_{-n}^* e^{-i\varphi} \right)$ which leads to the distortion of the detected line shape and the shift of the zero crossing from $\Delta = 0$ to $\Delta = \delta$. The amount of this frequency shift is obtained by solving

$$S_{det} = 0 , \qquad \text{(A8)}$$

that is to say, from (A7)

$$Re\{T_0\} Re\left\{ h_0 \left(h_n^* e^{i\varphi} + h_{-n}^* e^{-i\varphi} \right) \right\} - Im\{T_0\} Im\left\{ h_0 \left(h_n^* e^{i\varphi} + h_{-n}^* e^{-i\varphi} \right) \right\} = 0 . \qquad \text{(A9)}$$

For the Lorentzian line shape

$$T_0(\Delta) = \frac{1}{1 + i\dfrac{\Delta}{g}} \qquad \text{(A10)}$$

with a half width at half maximum $HWHM = g$, the solution of (A9) is

$$\delta = -g \frac{Re\left\{ h_0 \left(h_n^* e^{i\varphi} + h_{-n}^* e^{-i\varphi} \right) \right\}}{Im\left\{ h_0 \left(h_n^* e^{i\varphi} + h_{-n}^* e^{-i\varphi} \right) \right\}} . \qquad \text{(A11)}$$

The sensitivity of the pseudo-centre to the deviations of φ from φ_0 is

$$\left(\frac{\partial \delta}{\partial \varphi} \right)_{\varphi_0, \beta_0} = g \left(\frac{|h_0|^2 \left(|h_n|^2 - |h_{-n}|^2 \right)}{Re^2\left\{ h_0 \left(h_n^* - h_{-n}^* \right) \right\}} \right)_{\beta_0} \qquad \text{(A12)}$$

and that to the deviations of β from β_0 is

$$\left(\frac{\partial\delta}{\partial\beta}\right)_{\varphi_0,\beta_0} = -\frac{g}{2}\left(\frac{Im\left\{h_0\left(h_n^*-h_{-n}^*\right)\left[\left(h_{-1}^*-h_1^*\right)\left(h_n-h_{-n}\right)+h_0^*\left(h_{n-1}-h_{n+1}-h_{-n-1}+h_{-n+1}\right)\right]\right\}}{\left(Re\left\{h_0\left(h_n^*-h_{-n}^*\right)\right\}\right)^2}\right)_{\beta_0}. \quad \text{(A13)}$$

VI. References

[1] Bjorklund G C 1980 Frequency-modulation spectroscopy: a new method for measuring weak absorptions and dispersions *Opt. Lett.* **5** 15-17

[2] Bjorklund G C, Levenson M D, Lenth W, Oritz C 1983 Frequency-modulation (FM) spectroscopy: Theory of lineshapes and signal-to-noise analysis *Appl. Phys. B* **32** 145-152

[3] Hall J L, Hollberg L, Ma Long-Sheng, Baer T, Robinson H G 1981 Progress toward phase-stable optical frequency standards *J. Physique* **42(C8)** 59-71

[4] Hall J L, Hollberg L, Baer T, Robinson H G 1981 Optical heterodyne saturation spectroscopy *Appl. Phys. Lett.* **39** 680-682

[5] Drever R W, Hall J L, Kowalski V, Hough J, Ford G M, Munley A J, Ward H 1983 Laser phase and frequency stabilization using an optical resonator *Appl. Phys. B* **31** 97-105

[6] Whittaker E A, Gehrtz M, Bjorklund G C 1985 Residual amplitude modulation in laser electro-optic phase modulation *J. Opt. Soc. Am. B* **2** 1320-1326

[7] Lenth W 1984 High frequency heterodyne spectroscopy with current-modulated diode laser *IEEE J. Quant. Elect.* **20** 1045-1050

[8] Wong N C, Hall J L 1985 Servo control of amplitude modulation in frequency-modulation spectroscopy: demonstration of shot-noise-limited detection *J. Opt. Soc. Am. B* **2** 1527-1533

[9] du Burck F, Lopez O 2002 Stabilisation of laser beam intensity at 2.5 MHz *Electron. Lett.* **38** 1447-1449

[10] Kasapi S, Lathi S, Yamamoto Y 1997 Amplitude-squeezed, frequency-modulated, tunable, diode-laser-based source for sub-shot-noise FM spectroscopy *Opt. Lett.* **22** 478-480

[11] Kasapi S, Lathi S, Yamamoto Y 2000 Sub-shot-noise frequency-modulation spectroscopy by use of amplitude-squeezed light from semiconductor lasers *J. Opt. Soc. Am. B* **17** 275-279

[12] Gehrtz M, Lenth W, Young A T, Johnston H S 1986 High-frequency-modulation spectroscopy with lead-salt diode laser *Opt. Lett.* **11** 132-134

[13] Cooper D. E., Gallagher T F 1985 Double frequency modulation spectroscopy: high modulation frequency with low-bandwidth detectors *Appl. Opt.* **24** 1327-1334

[14] Janik G R, Carlisle C B, Gallagher T F 1986 Two-tone frequency-modulation spectroscopy *J. Opt. Soc. Am. B* **3** 1070-1074

[15] Werle P 1998 A review of recent advances in semiconductor laser based gas monitors *Spectrochim. Acta Part A* **54** 197-236

[16] Gehrtz M, Bjorklund G C, Whittaker E A 1985 Quantum-limited laser frequency-modulation spectroscopy *J. Opt. Soc. Am. B* **2** 1510-1526

[17] Bjorklund G C, Levenson M D 1981 Sub-Doppler frequency-modulation spectroscopy of I_2 *Phys. Rev.* **24** 166-169

[18] Arie A, Byer R L 1993 Laser heterodyne spectroscopy of $^{127}I_2$ hyperfine structure near 532 nm *J. Opt. Soc. Am. B* **10** 1990-1997; ERRATA 1994 *J. Opt. Soc. Am. B* **11** 866

[19] Bordé C J, Camy G, Decomps B 1979 Measurement of the recoil shift of saturation resonances of $^{123}I_2$ at 5145 Å: a test of accuracy for high-resolution saturation spectroscopy *Physical Review A* **20** 254-268

[20] du Burck F, Wallerand J-P, Goncharov A N, Himbert M, Bordé Ch J 1996 Recent progress in ultra-high resolution spectroscopy of molecular iodine *in Laser Spectroscopy XII, eds. M. Inguscio, M. Allegrini, A. Sasso (London:World Scientific)* 220-221
[21] Cheng W Y, Chen L, Yoon T H, Hall J L, Ye J 2002 Sub-Doppler molecular-iodine transitions near the dissociation limit (523-498 nm) *Opt. Lett.* **27** 571-573
[22] Hall J L, Robinson H G, Baer T, Hollberg L 1983 The lineshapes of subdoppler resonances observable with FM side-band (optical heterodyne) laser techniques *in Advances in Laser Spectroscopy eds F. T. Arecchi, F. Strumia and H. Walther (New York and London:Plenum Press)* 99-126
[23] Bava E, Massari F 1996 Phase sensitive detection of light reflected from a Fabry-Perot interferometer *Rev. Sci. Instrum.* **67** 1714-1720,.
[24] du Burck F, Wallerand J-P, Mercier B, Goncharov A N, Himbert M, Bordé C J 2001 Resolving power and sensitivity in modulation transfer stimulated resonant Raman spectroscopy *IEEE J. Quant. Elect.* **37** 837-843
[25] du Burck F, Wallerand J-P, Goncharov A N, Himbert M 2001 High frequency modulation transfer technique for ultra-high resolution spectroscopy of I_2 *IEEE Trans. Instrum. Meas.* **50** 493-496
[26] Bordé Ch J, Camy G, Decomps B, Descoubes J-P, Vigué J 1981 High-precision saturation spectroscopy of $^{127}I_2$ with argon lasers at 5145 Å and 5017 Å: I - Main resonances *J. Physique* **42** 1393-1411
[27] Camy G, Bordé C J, Ducloy M 1982 Heterodyne saturation spectroscopy through frequency modulation of the saturating beam *Opt. Comm.* **41** 325-330
[28] Taub H, Schilling D L 1986 *Principles of communication system, 2nd edition (New York:Mc Graw Hill Book Company)*

Figure captions

Fig. 1: Principle of FM spectroscopy.

Fig.2: Computed line shapes for a Lorentzian response of the sample ($HWHM = g$).
$n = 3;\ \beta = 3.544;\ \varphi = \pi/2;\ \mu = 0.3;\ \psi = 0$
(a) The solid lines are the components centred at $\Delta = -\omega_m$, 0 and $+\omega_m$ ($\omega_m = 10g$); The broken line is the sum of the three previous components.
A slight shift of the component centred at $\Delta = 0$ appears due to the components centred at $\Delta = \pm\omega_m$.
(b) Detected line shapes for various modulation frequencies ω_m computed from (11) without the dc background.

Fig.3: Experimental set up.
AOM1 and AOM2: acousto-optic modulators; BSC: polarizing beam splitter cube; PD1 and PD2: photodiodes; PS: power splitter, Opt. att.: optical attenuator, RF att. electrical attenuator.

Fig. 4: Third harmonic detection of the hyperfine component a_2 of the P(13) line of iodine at 514.5 nm. The modulation index is $\beta = 2.8$.
Iodine pressure: ~0.133 Pa (1 mTorr); saturating beam power: 1.5 mW; probe beam power: 0.17 mW; beams diameter: 6 mm; time constant: 300 ms; one sweep of 100 s.

Fig. 5: Third harmonic detection of the hyperfine component a_2 of the P(13) line of iodine at 514.5 nm. The modulation index is $\beta = \beta_0 = 3.544$.
Iodine pressure: ~0.066 Pa (0.5 mTorr); saturating beam power: 0.51 mW; probe beam power: 0.34 mW; beams diameter: 6 mm; time constant: 300 ms; one sweep of 100 s.

Fig. 6: Deviation of the pseudo-centre of the line δ versus the deviation from the ideal detection phase $\Delta\varphi = \varphi - \varphi_0$ for a modulation index β_0 ($\mu = 0.3$).
Squares: $\psi = 95°$; Circles: $\psi = 185°$. The solid lines are the theoretical deviations given by (A11). The broken lines are the theoretical deviations derived from (11).

Fig. 7: Deviation of the pseudo-centre of the line δ versus the deviation from the ideal modulation index $\Delta\beta = \beta - \beta_0$ for a detection phase φ_0 ($\mu = 0.3$).
Squares: $\psi = 95°$; Circles: $\psi = 185°$. The solid lines are the theoretical deviations given by (A11). The broken lines are the theoretical deviations derived from (11).

	$n = 1$	$n = 2$	$n = 3$	$n = 4$	$n = 5$	$n = 6$	$n = 7$
$K = 1$	-	-	3.544	3.146	2.963	2.855	2.782
$K = 3$	3.544	2.076	6.101	2.552	4.119	4.832	5.206
$K = 5$	2.964	5.288	4.119	7.312	11.988	3.782	4.852

Table 1: Some solutions of equation (A6)

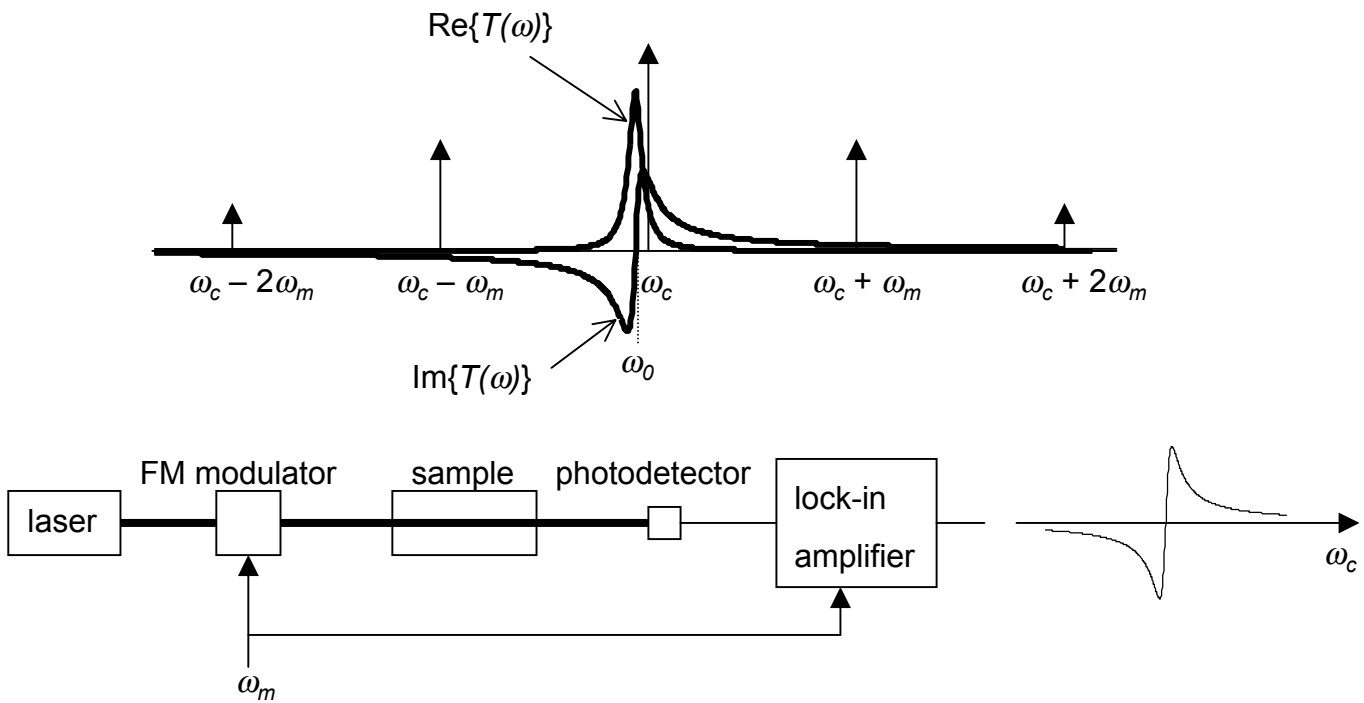
Re{T(ω)}
ω_c – 2ω_m
ω_c – ω_m
ω_c
ω_c + ω_m
ω_c + 2ω_m
Im{T(ω)}
ω_0
laser
FM modulator
sample
photodetector
lock-in
amplifier
ω_c
ω_m

Fig. 1

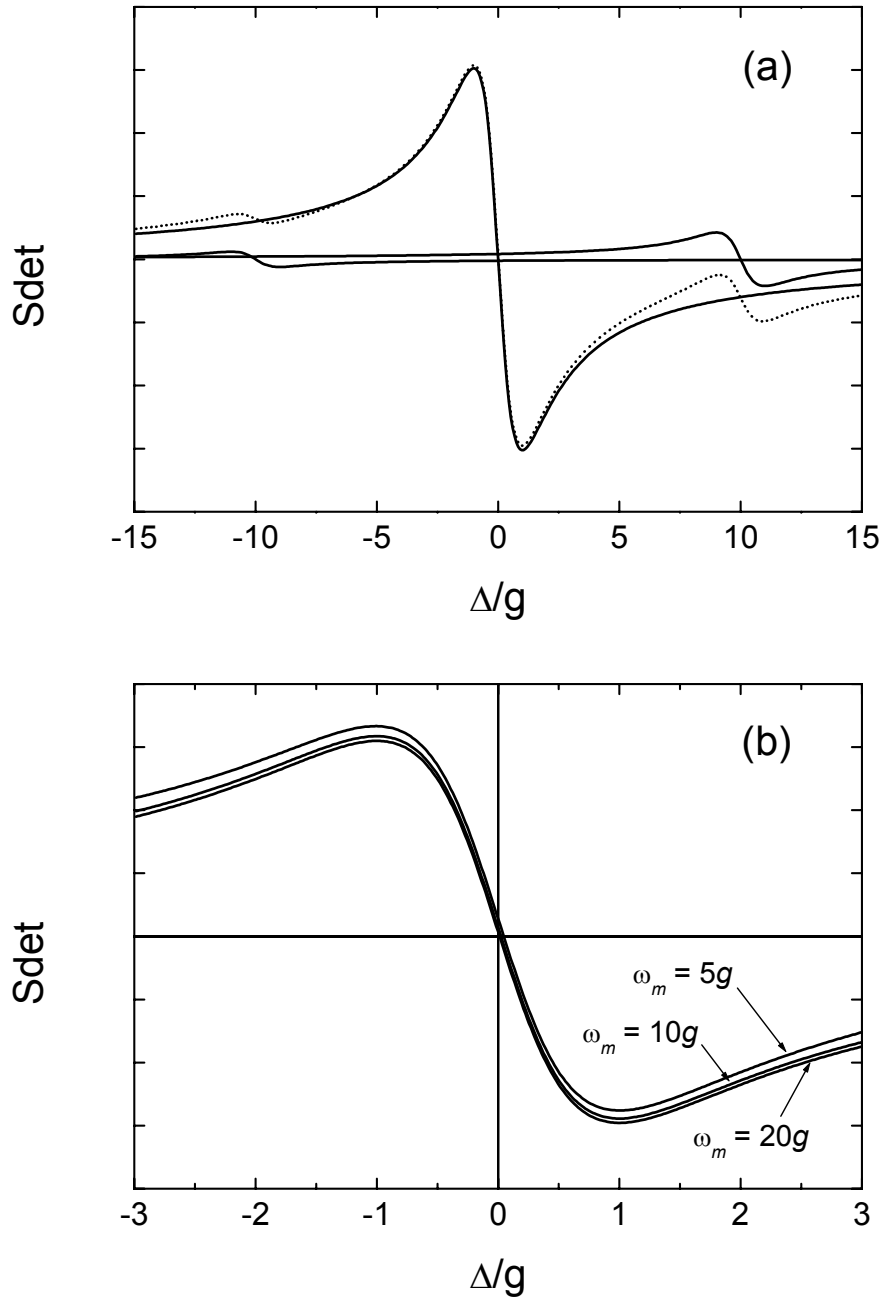

Fig. 2

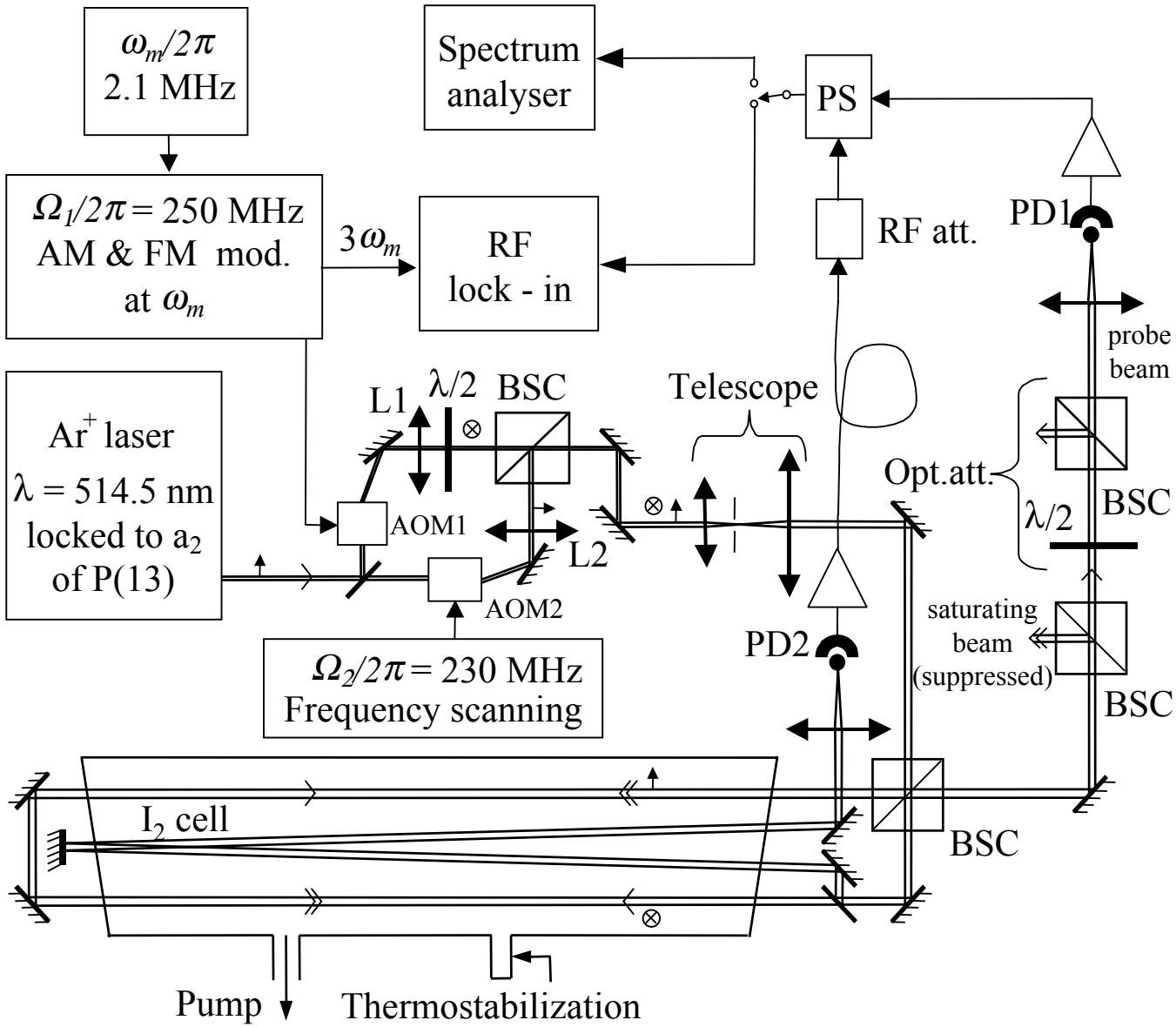
$\omega_m/2\pi$
2.1 MHz
Spectrum analyser
PS
$\Omega_1/2\pi = 250$ MHz
AM & FM mod.
at ω_m
$3\omega_m$
RF lock - in
RF att.
PD1
probe beam
Ar$^+$ laser
$\lambda = 514.5$ nm
locked to a_2
of P(13)
L1
$\lambda/2$
BSC
Telescope
AOM1
L2
AOM2
Opt.att.
$\lambda/2$
BSC
saturating beam (suppressed)
BSC
PD2
$\Omega_2/2\pi = 230$ MHz
Frequency scanning
I_2 cell
BSC
Pump
Thermostabilization

Fig. 3

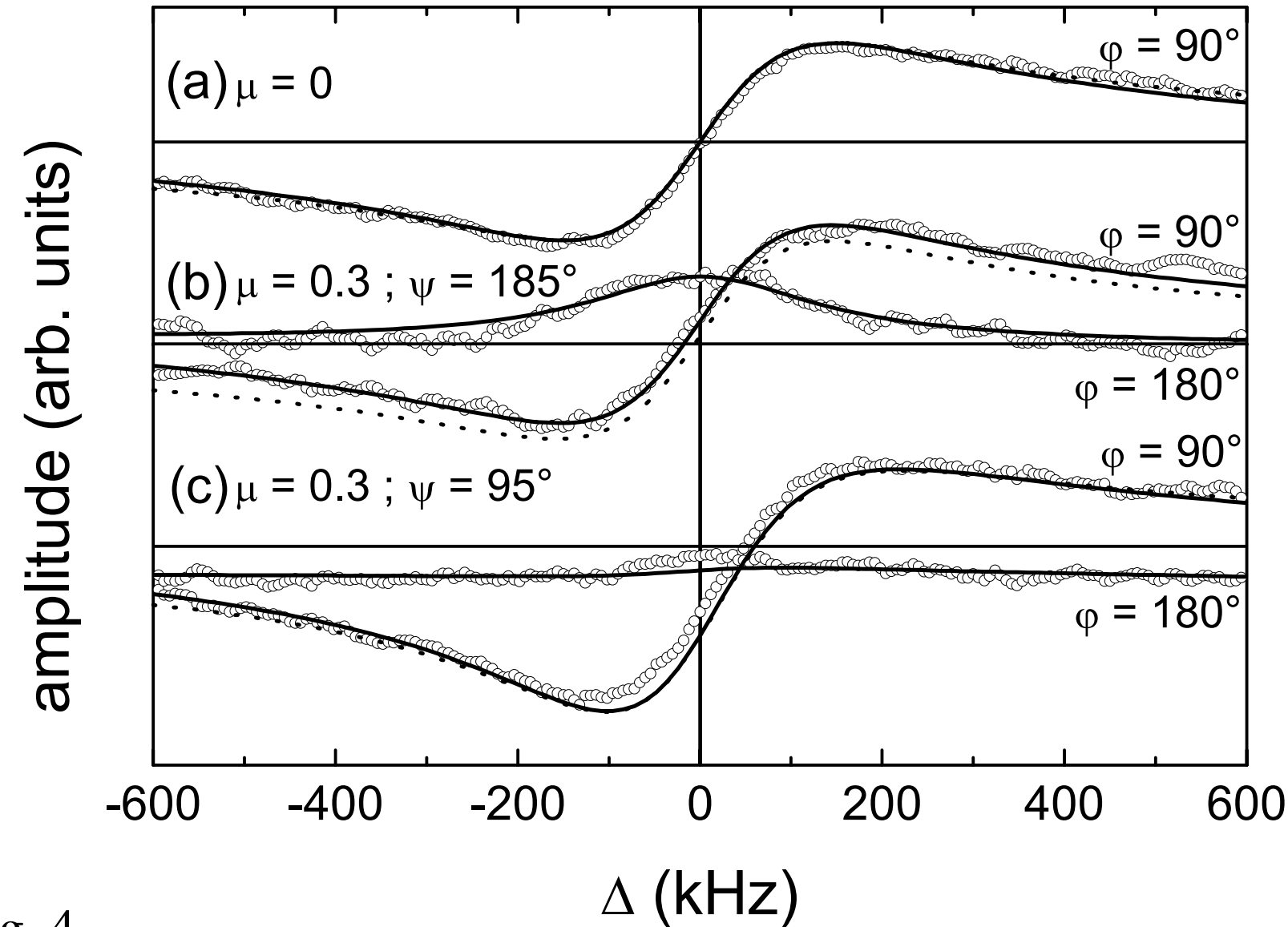
(a) μ = 0
φ = 90°
(b) μ = 0.3 ; ψ = 185°
φ = 90°
φ = 180°
(c) μ = 0.3 ; ψ = 95°
φ = 90°
φ = 180°
amplitude (arb. units)
-600
-400
-200
0
200
400
600
Δ (kHz)

Fig. 4

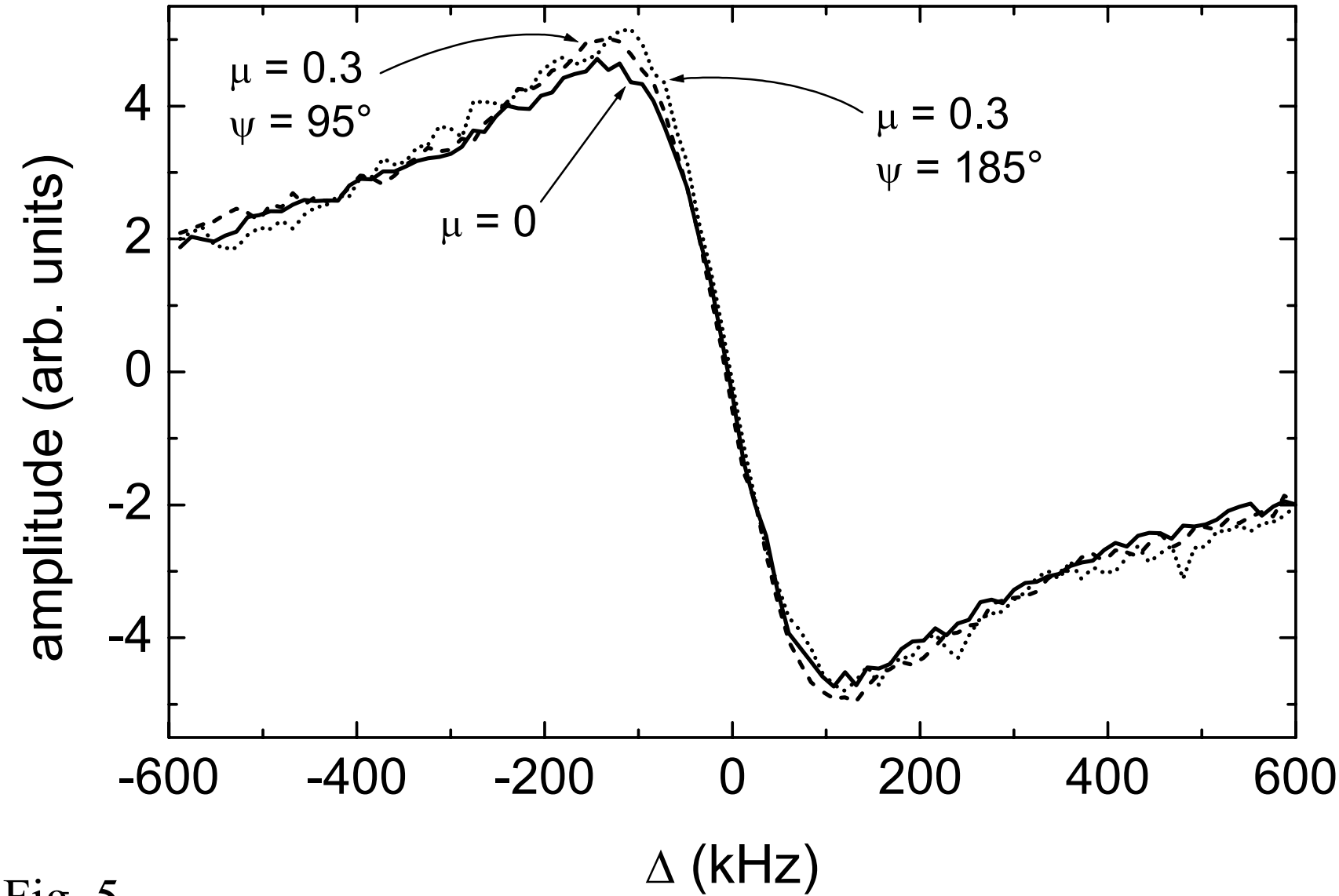
μ = 0.3
ψ = 95°
μ = 0
μ = 0.3
ψ = 185°
amplitude (arb. units)
4
2
0
-2
-4
-600
-400
-200
0
200
400
600
Δ (kHz)

Fig. 5

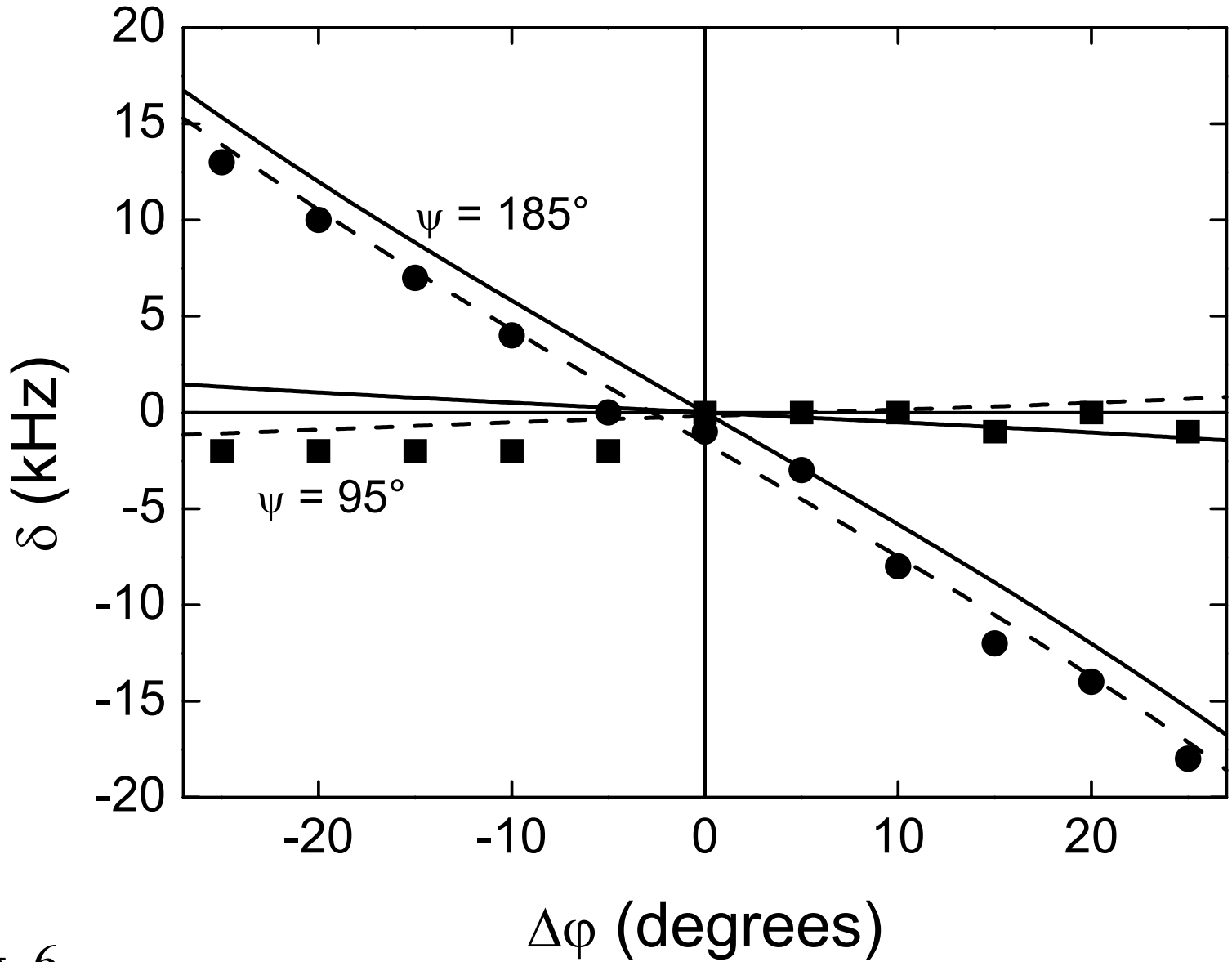

Fig. 6

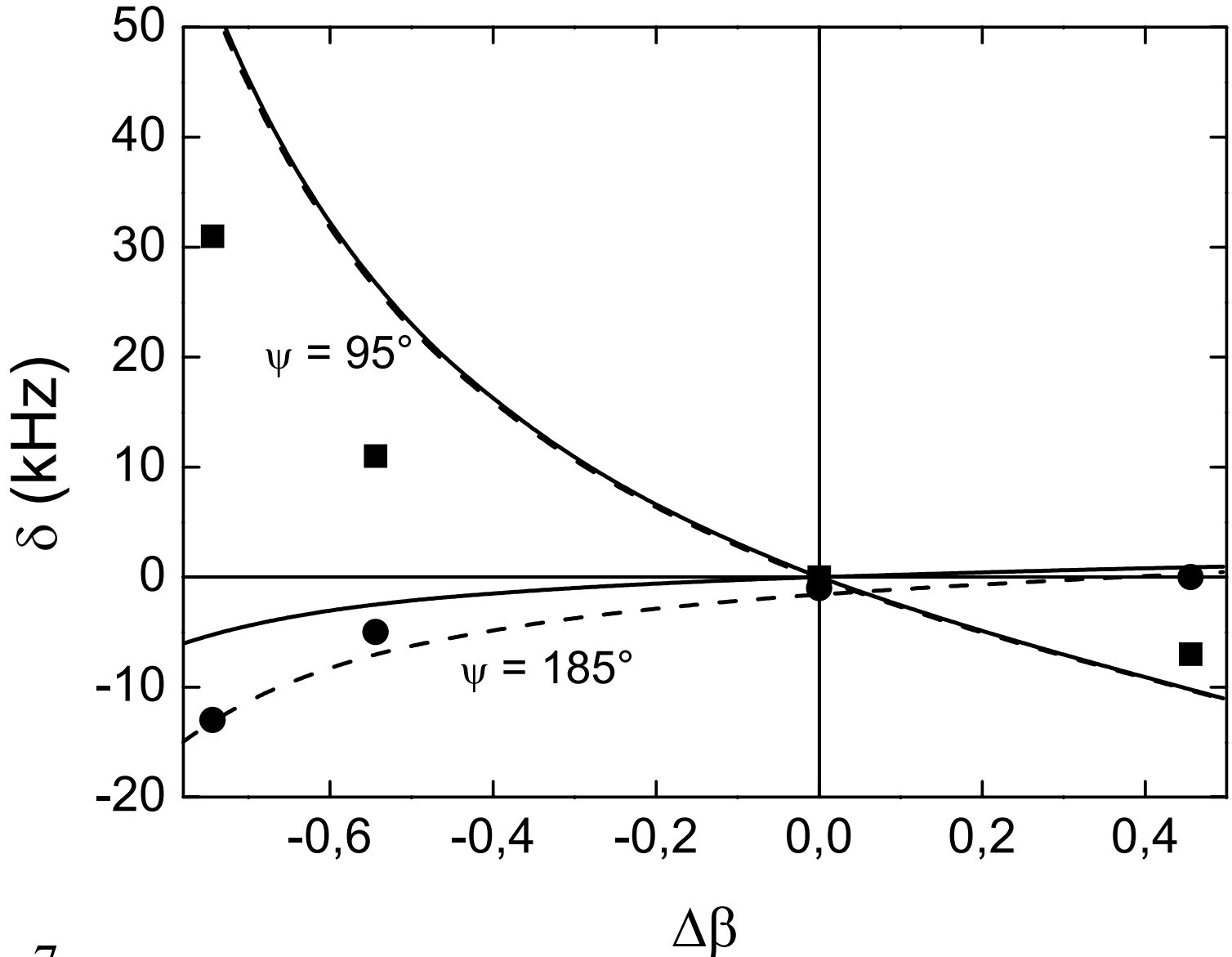

Fig. 7